Zhen Yang ✉
Qian Tang
Dong Peng
Zeyin He
Chun Gan

https://doi.org/10.21278/TOF.501071024
ISSN 1333-1124
eISSN 1849-1391

AN ANALYTICAL CALCULATION METHOD OF MULTI-TOOTH IMPACT OF HIGH-SPEED INVOLUTE HELICAL GEAR PAIR

Summary

This paper presents an analytical calculation method for high-speed helical gear multi-tooth impact excitation based on energy conservation considering the temperature effect. Firstly, considering the tooth surface contact temperature factor, the position of the meshing point of a gear tooth is determined. Then, the meshing impact excitation of the first pair of helical gears, considering the temperature effect, is obtained. Secondly, based on the principle of conservation of energy, the amount of change in the meshing speed of tooth pairs II and III, induced by the meshing impact excitation outside the line, is determined, and an analytical model for the impact of tooth pairs II and III is established; the model will obtain the impact excitation of tooth pairs II and III. Then, the evolution law of multi-tooth impact excitation induced by the meshing impact excitation is explained. Finally, the influence of gear impact on the time-varying friction excitation and the tooth surface load is studied. The proposed calculation method can accurately and quickly calculate the multi-tooth impact excitation of a high-speed helical gear pair and provide theoretical support for the prediction of the impact and contact state of a gear system in engineering practice.

Key words: *Involute helical gear; multi-tooth impact excitation; theoretical model; energy conservation; meshing state*

1. Introduction

The involute helical gear has the advantages of stable transmission, high bearing capacity, and convenient processing and adjustment. It has been extensively applied in aerospace applications, high-speed trains, wind power generation, and other high-speed occasional applications [1-2]. When the gear runs at high speed, the friction on the tooth surface generates a lot of heat, resulting in an increase in its temperature [3]. The tooth profile and meshing characteristics of the gear are changed to make the gear bear greater impact load, which affects the meshing state of the gear. Therefore, it has become necessary in the gear research field to accurately and efficiently calculate the gear impact, considering temperature.

So far, researchers have conducted extensive investigations into the gear meshing impact excitation mainly through the finite element method (FEM) [4-7], tooth contact analysis (TCA)/loaded tooth contact analysis (LTCA) [8-9], and analytical method (AM). The finite element method is extensively used because it can simulate the operating conditions of complex structures accurately. The researchers of the studies [10-11] established a numerical calculation model of the impact dynamics of gear pairs by means of the FEM and obtained the meshing impact as a result. The influence of the impact speed on the impact characteristics of the gear was analysed [12]. The stress distribution of the gear during impact was studied [13]. In solving the meshing impact using TCA/LTCA, the researchers of the studies [14-15] calculated the meshing stiffness and the position of the initial meshing point according to the same analyses and obtained the meshing impact force. The influence of input speed and load on the meshing impact was studied in [16]. However, when the finite element method and tooth contact/loaded tooth contact analyses are used to solve the meshing impact force, it is inevitable to conduct modelling and setting operations, which increases the time cost of calculation, and the efficiency is relatively low. Thus, this method cannot meet the requirements of rapid design in the product development process. Therefore, some researchers have focused on the more efficient analytical method to obtain the meshing impact force, the position of the initial meshing considering the gear load deformation, and other factors. A meshing impact dynamic model has been established. The meshing impact excitations of spur gear [17-18], double circular arc gear [19], and helical gear [20] were calculated, and the influence of gear geometric parameters on the meshing impact was analysed [21]. Many valuable research results have been obtained in the analytical calculation of the meshing impact force.

However, the authors found that the meshing impact excitation outside the line will lead to a sudden change in the gear linear speed, resulting in a speed difference that induces impact excitation between other meshing tooth pairs. Therefore, the gear meshing process is a multi-tooth impact process that changes the meshing state of a gear pair. Although there is an analytical model for the meshing impact of the involute helical gear [20], it only considers the impact of meshing teeth on single teeth, and the problems of adjacent tooth impact and temperature effect are not considered. Considering the temperature effect, there are few reports on the phenomenon of gear multi-tooth impact induced by the meshing impact and the change in the gear meshing state.

Therefore, our group proposes a calculation method for the multi-tooth impact excitation of a helical gear based on energy conservation considering the temperature effect, and analyses the influence of gear impact on the gear meshing state; this provides theoretical support for accurate and rapid calculation of helical gear pair excitation.

2. Calculation of the meshing impact excitation of a helical gear pair considering temperature

The principle of meshing impact is shown in Figure 1. The tooth pitches of the driving gear and the driven gear are p_{b1} and p_{b2}, respectively; under ideal conditions, the two tooth pitches are equal. In actual meshing, due to the influence of factors such as elastic deformation of teeth, they are not, i.e., $p_{b1} \neq p_{b2}$. The difference between the tooth pitches is indicated by Δp in the figure. This difference will produce a normal impact speed and the meshing impact excitation outside the line of action. Numerous valuable research results have been obtained in the analytical calculation of the meshing impact force [22]. The tooth surface temperature leads to the thermal deformation of the gear, which aggravates the meshing impact of the gear pair. In the figure, ω_1 is the rotational angular velocity of the driving gear.

The tooth surface temperature causes thermal deformation of the gear. According to Ref. [23], the thermal deformation, δ_T, can be expressed as follows:

$$\delta_T = \frac{-T_f \lambda r_b \left(r_b + u_b\right)}{2\left[r_b + u_b \cos\alpha_c + T_f \lambda r_b \left(1 - \cos\alpha_c\right)\right]} \times \left[\frac{S}{r} - 2\left(\text{inv}\alpha_c - \text{inv}\alpha\right)\right]$$
$$T_f = \frac{\mu F_n v_s}{\sqrt{\pi\lambda c \rho b v_e}}, \tag{1}$$

where λ is the expansion coefficient of the material, T_f is the flash temperature of the tooth surface, r_b is the base circle radius, α_c is the pressure angle after thermal deformation, α is the pressure angle, S is the tooth thickness on the pitch circle, r is the pitch circle radius, F_n is the normal load of the tooth surface, v_s is the relative sliding speed, c is the specific heat capacity of the material, ρ is the material density, b is the contact half width, v_e is the entrainment velocity, and u_b is the base circle thermal deformation. The latter can be expressed as

$$u_b = \lambda r_b T\left(r_0\right) + \frac{1+\upsilon}{1-\upsilon} \times \frac{\lambda r_b \left(r_b^2\left(1-2\upsilon\right) - r_0^2\right)}{r_b^2 - r_0^2} \times \left(T\left(r_b\right) - T\left(r_0\right)\right), \tag{2}$$

where v is Poisson's ratio, r_0 is the radius of the gear shaft, $T(r_b)$ and $T(r_0)$ are the temperature of the gear shaft and the base circle, respectively.

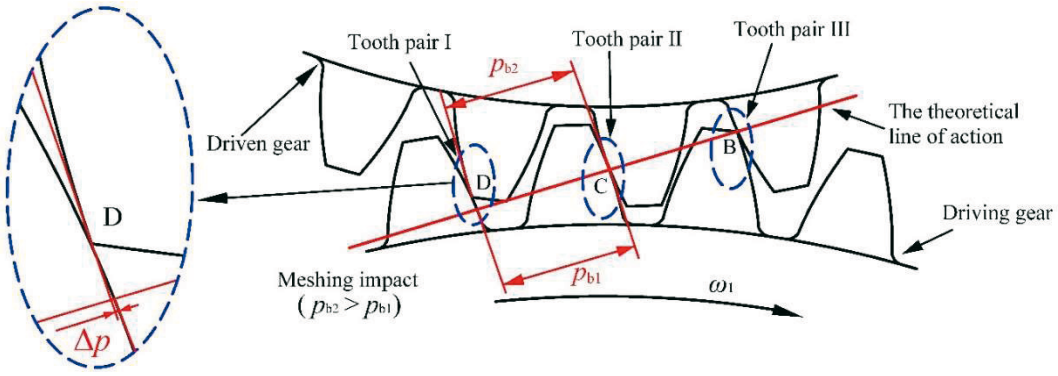

Fig. 1 Principle of the meshing impact

According to the reversal method, the driving and driven gears are reversed by θ_1 and θ_2 respectively, as shown in Fig. 2. According to the geometric relationship in the figure, the following expressions are valid:

$$r_{O_1D} = \sqrt{r_{a2}^2 + a^2 - 2 r_{a2} a \cos(\varphi + \theta_2 + \gamma_2)} \tag{3}$$

$$\delta_\Sigma = \delta_1 + \delta_2 + \delta_c + \delta_{T1} + \delta_{T2} \tag{4}$$

$$\varphi = \delta_\Sigma / \left(r_{b2} + u_{b2}\right) \tag{5}$$

where r_{O_1D} represents the impact radius of meshing point D, a represents the centre distance, r_{a2} is the addendum circle radius of the driven gear; other parameters are listed in Ref. [20].

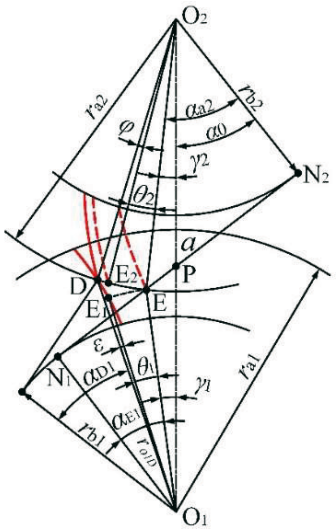

Fig. 2 Schematic diagram of the meshing impact point

The impact radius of meshing point D is obtained by solving the above equations.

As shown in Fig.3, the helical gear is divided into a number of independent spur gears by the slice method; the slice thickness is expressed as Δx. The impact excitation of a helical gear can be obtained by adding together the meshing impact excitation of each slice spur gear. From the results presented in the previous literature, this method is feasible. Figure 3 shows the instantaneous speed of the i-th spur gear at the impact point D_i. The instantaneous meshing speeds of different sliced master and follower gears are denoted by v_{1i} and v_{2i}, respectively, and the speed difference Δv_{ni} of the gear pair in the instantaneous meshing line is obtained by projecting them onto the meshing line. The speed difference between the two speeds in the direction of the normal of the instantaneous meshing line is expressed as $\Delta v_{\tau i}$. Thus, the impact velocity Δv_{ni} of the ith spur gear can be obtained as follows:

$$\Delta v_{ni}=v_{1i}-v_{2i}=\omega_1 r_{b1}-\omega_2 r'_{b2i} \tag{6}$$

$$r'_{b2i}=a\cos\left(\arccos\left(r_{b1}/r_{O_1Di}\right)+\varepsilon_i+\theta_i+\gamma_1\right)-r_{b1}, \tag{7}$$

where ω_1 and ω_2 denote the angular speeds of the driving and driven gears, respectively, and r'_{b2i} denotes the instantaneous base circle radius of any spur driven gear.

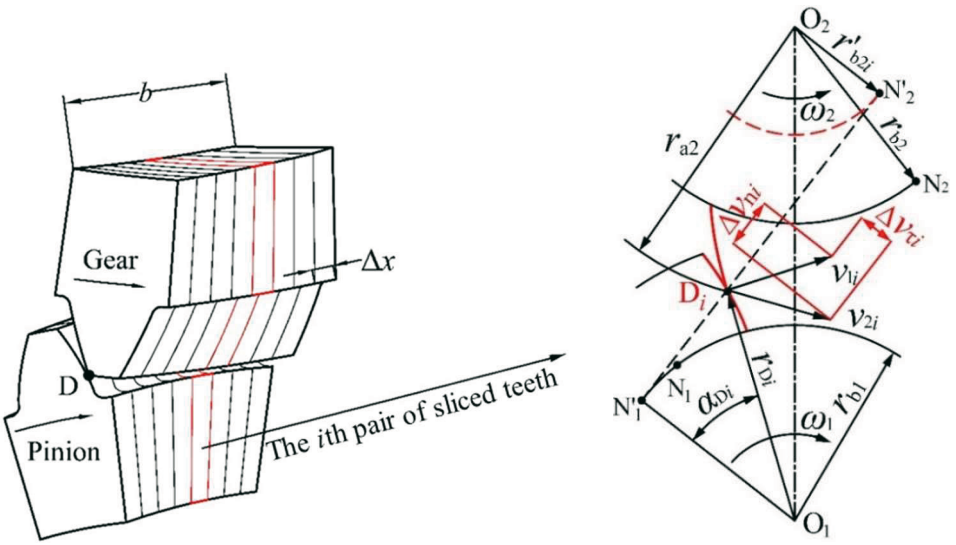

Fig. 3 Speed of meshing impact position D

Based on the impact mechanics theory, the maximum impact force of any spur gear F_{si} can be expressed as (see reference [18] for details):

$$F_{si} = \Delta v_{ni} \sqrt{\frac{\Delta x J_{1i} J_{2i}}{\left(J_{1i} r'^2_{b2i} + J_{2i} r^2_{b1}\right) q_{si}}} \ , \tag{8}$$

where $\Delta x = b/N$ represents the slice thickness, and N represents the slice number; J_{1i} and J_{1i} denote the moment of inertia of the driving and driven gears, respectively, while q_{si} represents the comprehensive flexibility of any spur gear pair at the meshing impact position.

The maximum meshing impact force of tooth pair I, F_{sm1}, is calculated by adding together the maximum impact force of all spur gears; it can be expressed as

$$F_{sm1} = \sum F_{si} \ . \tag{9}$$

It is assumed that the change law of meshing impact is a sinusoidal function, and the following relation is satisfied for the meshing impact excitation formula of tooth pair I:

$$F_{s1}(t) = F_{sm1} \sin\left(\pi t / t_{s1}\right) = F_{sm1} \sin \omega_{s1} t \ , \tag{10}$$

where $\omega_{s1} = \pi / t_{s1}$ denotes the impact angular frequency and t_{s1} denotes the impact time, that is, the process in which the impact velocity decreases from v_n to 0. According to the impulse theorem, the impact time t_{s1} can be expressed as

$$t_{s1} = \frac{\pi}{2} \frac{m_{red} \Delta v_n}{F_{sm1}} \ , \tag{11}$$

where m_{red} denotes the equivalent mass of the sliced spur gear, and Δv_n represents the maximum gear impact speed of the sliced spur gear.

3. Multi-tooth impact analytical calculation of a helical gear induced by meshing impact

Since the meshing impact of tooth pair I only occurs on one side of the tooth width, the speeds of the driving and driven gears on the impact side slightly fluctuate, resulting in a speed difference, which induces the impact of meshing tooth pair II and tooth pair III. According to the principle of energy conservation and the slice method, the maximum impact force of tooth pair II and tooth pair III induced by the meshing impact outside the line of action of tooth pair I is calculated.

3.1 Calculation of the gear tooth speed difference induced by meshing impact

Due to the meshing impact, the normal energy E_k is generated by the normal impact force, which will be transmitted from the driving gear to the driven gear. Therefore, the normal impact energy, E_k, can be expressed as

$$E_k = \sum \frac{1}{2} \frac{J_{1i} J_{2i}}{\left(J_{1i} r'^2_{b2i} + J_{2i} r^2_{b1}\right)} \Delta v^2_{ni} \ . \tag{12}$$

The tangential impact force produces the tangential impact energy, W_f, which will be lost through friction work; the energy loss of the driving gear can be expressed as

$$W_f = \sum \frac{1}{2} \frac{J_{1i} J_{2i}}{\left(J_{1i} r'^2_{b2i} + J_{2i} r^2_{b1}\right)} \Delta v^2_{\tau i} \tag{13}$$

$$\Delta v_{\tau i} = v'_{2i} \sin \beta'_i - v_{2i} \sin \beta_i \ , \tag{14}$$

where $\Delta v_{\tau i}$ represents the tangential impact speed of any spur gear, v_{2i} and v'_{2i} represent the linear speeds before and after the impact of the driven gear, respectively, and β_i and β_i' represent the angles between v_{2i} and v'_{2i} and the instantaneous meshing line before and after the impact, respectively.

Figure 4 is the process analysis diagram of gear speed change induced by tooth pair impact. The slice method is used to analyse the impact and the non-impact side. Meshing impact occurs on one side of the gear, resulting in different speeds on both sides of the gear. Subsequently, the speed of the driving gear on the impact side decreases, and the speed of the driven gear increases. The speed of the driving gear and the driven gear is v'_1 and v'_2, respectively, after the impact of tooth pair I. The speed of the other side remains unchanged, and the driving and the driven gear maintain the original speeds, v_1 and v_2. The helical gear is cut into N spur gears along the axial direction based on the slice theory. As shown in the lower right corner of the figure, the speeds of any spur gear can be described as follows:

$$\begin{cases} v'_{1i} = v'_1 + \dfrac{v_1 - v'_1}{\mathrm{N}-1}(i-1),\ i = 1,2,3\cdots N \\ v'_{2i} = v'_2 + \dfrac{v_2 - v'_2}{\mathrm{N}-1}(i-1),\ i = 1,2,3\cdots N \end{cases} \tag{15}$$

According to the principle of energy conservation, the speeds of the driving and driven gears after the meshing impact can be expressed as

$$\begin{cases} \dfrac{1}{2} m_{\mathrm{red1}} v_1^2 - \left(E_{\mathrm{k}} + W_{\mathrm{f}}\right) = \dfrac{1}{2}\sum m_{\mathrm{red1}i} v'^2_{1i} \\ \dfrac{1}{2} m_{\mathrm{red2}} v_2^2 + E_{\mathrm{k}} = \dfrac{1}{2}\sum m_{\mathrm{red2}i} v'^2_{2i} \end{cases}, \tag{16}$$

where m_{red1} and m_{red2} denote the equivalent masses of the driving and driven gears on the instantaneous meshing line, respectively, and $m_{\mathrm{red1}i}$ and $m_{\mathrm{red2}i}$ denote the equivalent masses of any spur driving and driven gears on the instantaneous meshing line, respectively.

There will be a backlash between the driving and driven gears on the impact side due to the change in speed. The lower left corner of the figure is the sectional view of tooth pair II on the meshing contact line. Assuming that during the impact the gear moves in a uniform variable motion, the maximum gear backlash $L_{\max}$ can be expressed as

$$L_{\max} = \frac{(v'_2 + v_2)t_{\mathrm{s1}}}{2} - \frac{(v_1 + v'_1)t_{\mathrm{s1}}}{2}\ . \tag{17}$$

Gear backlash is generated on one side of the meshing impact, and it is zero on the other side, assuming that the gear backlash changes linearly along the gear width direction. The gear backlash of any spur gear L_i can be described as

$$L_i = L - \frac{L}{N-1}(i-1)\,. \tag{18}$$

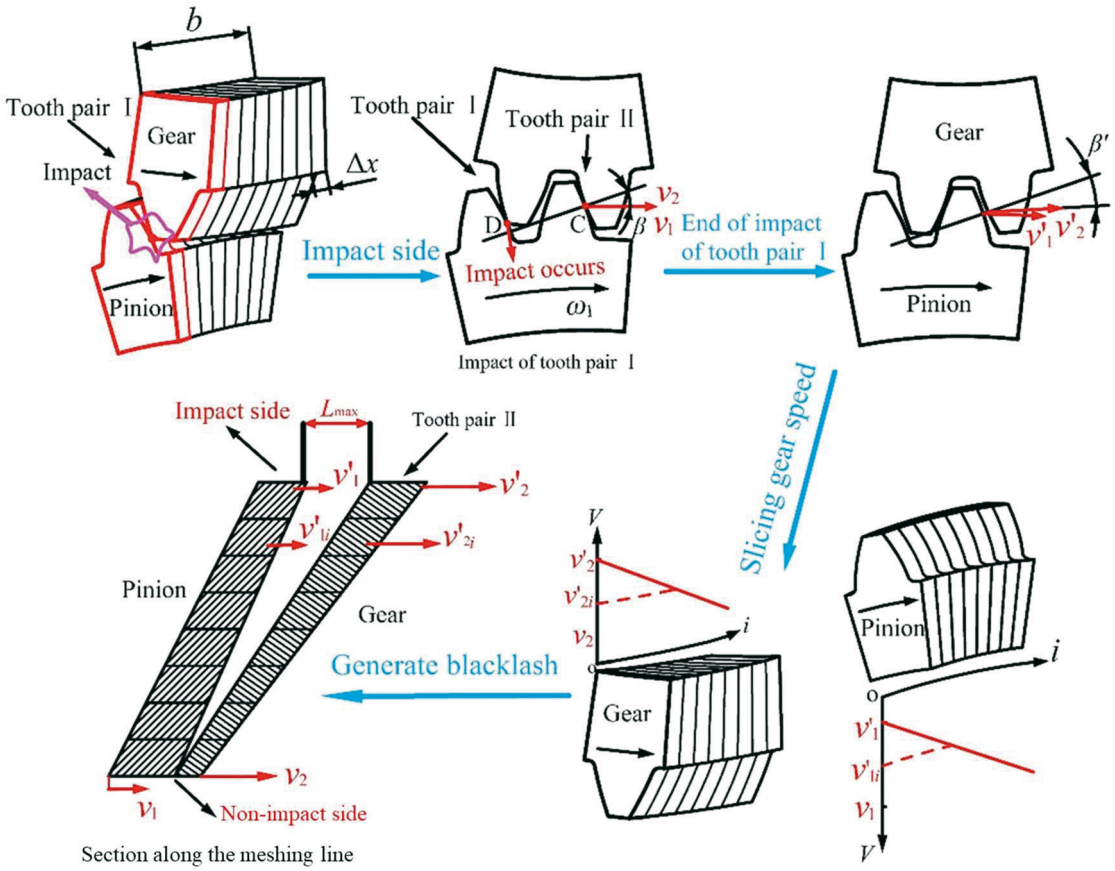

Fig. 4 Gear speed change after the impacts

3.2 Calculation of impact excitation

It is important to calculate the impact action line length accurately to solve the impact excitation. Figure5 shows the impact action lines of tooth pair II and tooth pair III on the meshing surface; it is possible to obtain the length of the impact action line.

The impact action lines of tooth pair II and tooth pair III are the positions after the impact of tooth pair I. The following relations are satisfied for the impact action line lengths of tooth pair II and tooth pair III:

$$\begin{cases} L_2 = \left(p_{\mathrm{bt}} + \omega_1 t_s r_{\mathrm{b1}} - \theta_1 r_{\mathrm{b1}}\right) / \sin\beta_{\mathrm{b}} \\ L_3 = B / \cos\beta_{\mathrm{b}} - \left(2p_{\mathrm{bt}} + \omega_1 t_s r_{\mathrm{b1}} - L_{\mathrm{EF}} - \theta_1 r_{\mathrm{b1}}\right) / \sin\beta_{\mathrm{b}} \end{cases}, \tag{19}$$

where p_{bt} denotes the circular pitch of the end face, and L_{EF} represents the actual meshing line length, i.e., $L_{\mathrm{EF}}=r_{\mathrm{b1}}(\tan\alpha_{\mathrm{a1}}-\tan\alpha_{\mathrm{E1}})$.

It is assumed that the driving gear and the driven gear are uniformly accelerated before recontacting; then, the speed of the driving and driven gears can be expressed as

$$\begin{cases} v_{1i} = v'_{1i} + a_1 t_i \\ v_{2i} = v'_{2i} - a_2 t_i \end{cases}, \tag{20}$$

where a_1 and a_2 denote the acceleration of the driving and driven gears, respectively; a_1 is equal to F_t/m_{red1}, a_2 is equal to F_t/m_{red2}, and t_i denotes the time for the gear pair to impact again; t_i can be obtained from the following formulae:

$$\begin{cases} x_{1i} = v'_{1i}t_i + \dfrac{1}{2}a_1 t_i^2 \\ x_{2i} = v'_{2i}t_i - \dfrac{1}{2}a_2 t_i^2 \end{cases}, \tag{21}$$

where x_{1i} and x_{2i} denote the moving distance of each driving gear and driven gear before contacting again, and x_{1i}-x_{2i}=L_i.

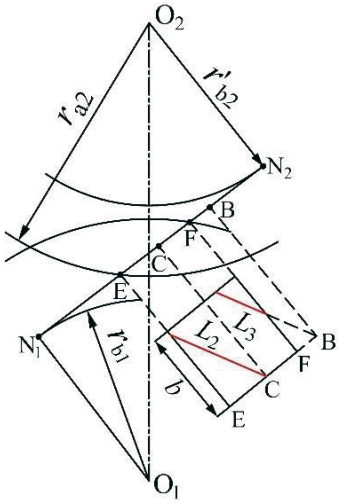

Fig. 5 Impact action line lengths

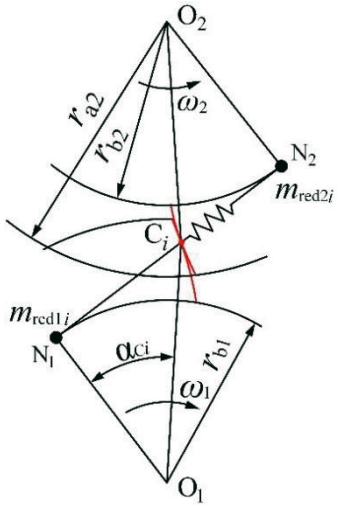

Fig. 6 The impact dynamic model of tooth pair II

Due to the gap between the driving and driven gears at the meshing position, the linear speed of the driving gear increases after acceleration, resulting in a relative speed difference and the meshing impact speed. The impact speed of any spur gear pair v_{si} can be obtained as follows:

$$v_{si} = v_{1i} - v_{2i} \tag{22}$$

Figure 6 shows the gear impact dynamic model. The meshing impact process of the driving and driven gears at point C_i approximates the elastic collision behaviour along line N_1N_2. The driving and driven gears are simplified as particles. Based on the impact mechanics theory, the maximum impact force F_{si}, the impact energy E_{ki}, and the maximum deformation are obtained as δ_{si} relationships. Therefore, the following relation is satisfied for the maximum impact force, (F_{si}), of any spur gear:

$$F_{si} = v_{si}\sqrt{\frac{\Delta x J_{1i} J_{2i}}{\left(J_{1i}r_{b2i}^2 + J_{2i}r_{b1}^2\right)q_{si}}} \tag{23}$$

The maximum impact force of tooth pair II, F_{sm2}, is calculated by summing the maximum impact force of all spur gears; it can be expressed as

$$F_{sm2} = \sum F_{si}\,. \tag{24}$$

It is assumed that the change law of the meshing impact is a sinusoidal function, and the following relation is satisfied for the impact excitation formula of tooth pair II:

$$F_{s2}(t) = F_{sm2}\sin\left(\pi t / t_{s2}\right) = F_{sm2}\sin\omega_s t \tag{25}$$

The impact excitation of tooth pair III, F_{s3}, is obtained according to the above method. Table 1 shows the parameters of the helical gear pair. The above analytical calculation method is compiled into a calculation program, and the impact excitation is calculated within a few minutes, which reflects the rapidity of the analytical method; this is also one of the advantages of the calculation method.

Table 1 The parameters of the helical gear pair

Parameter type	Driving gear	Driven gear
Number of teeth, z	41	161
Normal modulus, m_n / mm	12	12
Normal pressure angle, α_n / (°)	20	20
Helix angle, β / (°)	12	-12
Tooth width, B / mm	180	180
Addendum coefficient, h_{an}	1	1
Tip clearance coefficient, c_n	0.4	0.4
Input speed, n / (r·min^{-1})	3000	
Input power, P / (kW)	2720	

Figure 7 shows the multi-tooth impact excitation of the involute helical gear pair. The maximum impact value of tooth pair I, considering temperature, is 8264.7 N, and the maximum impact value of tooth pair I, without considering temperature, is 7114.3 N; the former shows an increase of 13.92%. The maximum impact value of tooth pair II, considering temperature, is 3460.9 N, and the maximum impact value, without considering temperature, is 3092.2 N; the former shows an increase of 10.65%. The maximum impact value of tooth pair III, considering temperature, is 1573.5 N, and the maximum impact value, without considering temperature, is 1406.1 N; the former shows an increase of 10.64%. Therefore, the tooth surface temperature increases the impact excitation of the helical gear pair, and the temperature has a great influence on the meshing impact of the helical gear pair. The impact of tooth pairs II and III is less affected by temperature than that of tooth pair I.

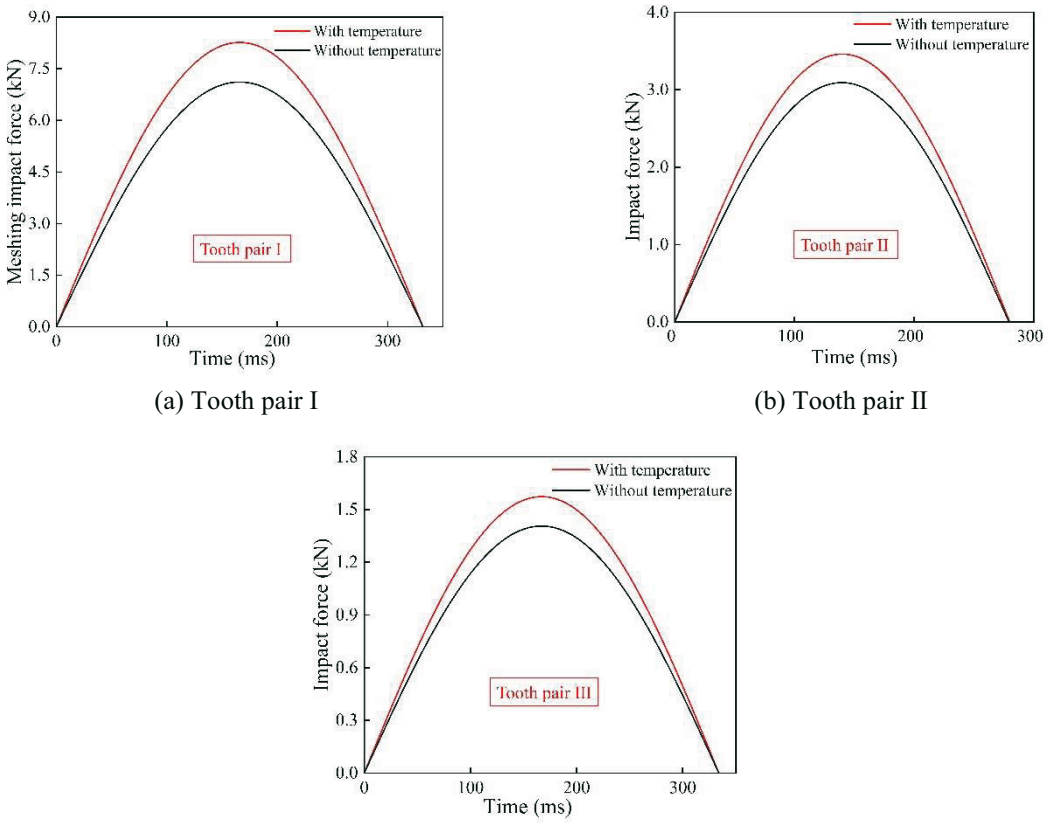

(a) Tooth pair I

(b) Tooth pair II

(c) Tooth pair III

Fig. 7 Impact excitation of each meshing tooth pair of the involute helical gear pair.

3.3 Multi-tooth impact characteristics

The influence of different gear parameters on the impact excitation of an involute helical gear pair is studied. Figure 8 shows the influence of different gear parameters on the impact force of the involute helical gear studied.

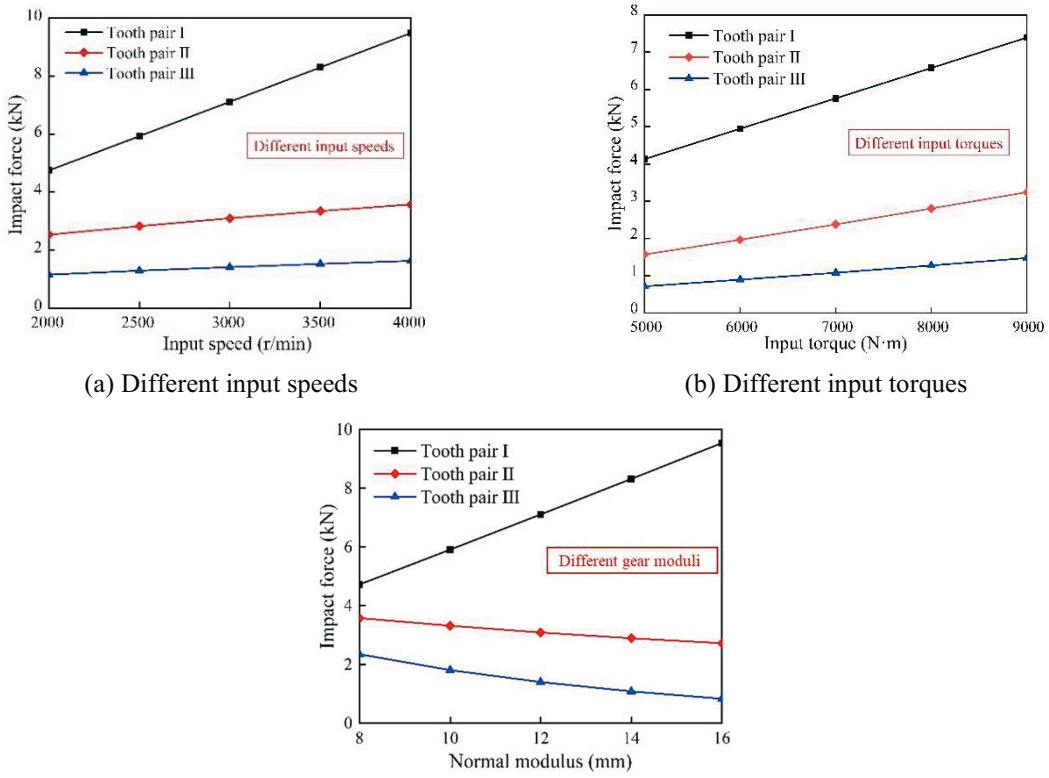

(a) Different input speeds

(b) Different input torques

(c) Different input moduli

Fig. 8 The multitooth impact excitation of the involute helical gear varying with parameters.

As the input speed increases, the impact speed of the gear increases, which enhances the meshing impact of the helical gear and also increases the impact of tooth pair II and tooth pair III. As the input torque increases, the impact force, F_n, on the unit tooth width of the helical gear increases, which enhances the multi-tooth impact excitation of the gear pair. As the gear modulus increases, the impact radius increases, resulting in the increase in the impact speed; this enhances the meshing impact of the helical gear. However, as the gear modulus increases, the gear mass increases, the influence of the meshing impact on the stability of the gear transmission system decreases, the gear speed fluctuation caused by the meshing impact decreases, and the impact of tooth pair II and tooth pair III is reduced.

4. Calculation method of time-varying friction excitation and tooth surface load considering gear impact

4.1 Calculation method of time-varying friction excitation considering gear impact

Due to the intervention of meshing impact outside the line of action, the oil film of the gear in the meshing stage breaks, which makes the tooth surfaces of the driving and driven gears come into direct contact and increases the sliding friction force. Now the helical gear is divided into three friction states in the complete meshing range: impact friction, mixed lubrication, and elastohydrodynamic lubrication (EHL). The impact friction takes place in the phase of meshing impact outside the line of action, in which the impact is the most intense. The tooth surfaces of the driving and driven gears are in direct contact. The mixed lubrication occurs

in the impact stage within the line of action, that is, in the process from the end of the impact outside the line to the reduction of the impact. In this stage, the lubrication state recovers from the initial impact friction state to the elastic lubrication state. Therefore, it is expressed in the form of the weighted sum of the EHL friction coefficient and the impact friction coefficient. The EHL state means that the gear lubrication returns to the normal level; its friction coefficient is calculated by the calculation method proposed by Xu [24].

(1) impact friction

The impact destroys the lubricating oil film on the tooth surface, resulting in the impact friction state of the meshing gear. The impact friction coefficient is obtained by the ratio of tangential impulse to normal impulse during the impact outside the line of action, and the impact friction coefficient can be expressed as

$$\mu_{\mathrm{I}}=\frac{\int_0^{t_{\mathrm{s}}} F_{\mathrm{I}\tau}\mathrm{d}t}{\int_0^{t_{\mathrm{s}}} F_{\mathrm{In}}\mathrm{d}t} \tag{26}$$

$$\begin{cases} m_{\mathrm{red}}\Delta V_{\mathrm{D2}\tau}=\int_0^{T_{\mathrm{s}}} F_{\mathrm{I}\tau}\mathrm{d}t \\ m_{\mathrm{red}}\Delta V_{\mathrm{D2n}}=\int_0^{T_{\mathrm{s}}} F_{\mathrm{In}}\mathrm{d}t \end{cases} \tag{27}$$

Taking formulae (26) and (27) simultaneously, the impact friction coefficient can be obtained as follows:

$$\mu_{\mathrm{I}}=\frac{\Delta V_{\mathrm{D2}\tau}}{\Delta V_{\mathrm{D2n}}}, \tag{28}$$

where $V_{\mathrm{D2}\tau}$ is the tangential impact velocity and V_{D2n} is the normal impact velocity.

As can be seen from Fig. 2, the impact outside the line of action is from point D to point E, so the time of the impact friction state can be expressed as

$$t_{\mathrm{I}}=\frac{\theta_1+\varepsilon}{\omega_1}\ . \tag{29}$$

(2) elastohydrodynamic lubrication

Under the condition of EHL, the sliding friction coefficient is calculated based on the calculation method proposed by Xu [24]. The Carreau lubricating oil is used in this paper. (See literature [25] for its parameters).

$$\mu_{\mathrm{EL}}\left(t\right)=e^{f\left(SR(t),P_{\max},\eta_0,S\right)}P_{\max}^{b_2}\left|SR\left(t\right)\right|v_e\left(t\right)^{b_6}\eta_0^{b_7}R\left(t\right)^{b_8} \tag{30}$$

$$\begin{aligned} f\left(SR\left(t\right),P_{\max},\eta_0,S\right)=b_1+b_4\left|SR\left(t\right)\right|P_{\max}\log_{10}\left(\eta_0\right) \\ +b_5e^{-\left|SR(t)\right|P_{\max}\log_{10}\left(\eta_0\right)}+b_9e^{R_{\mathrm{a}}} \end{aligned} \tag{31}$$

where $SR_m(t)$ denotes the slide-to-roll ratio, $P_{\max}$ denotes the maximum Hertzian pressure, η_0 denotes the absolute viscosity at oil inlet temperature, $R(t)$ denotes the effective curvature radius, R_{a} denotes the surface roughness, and $v_{\mathrm{e}}(t)$ denotes the entraining velocity.

(3) mixed elastohydrodynamic lubrication

Mixed EHL analysis typically requires the use of Reynolds equation, energy equation, Laplace equation, and elasticity equation [26]. In order to improve the solving efficiency, the friction coefficient of mixed EHL can be described by the weighted sum of EHL friction coefficient and impact friction coefficient according to the ISO standard.

$$u_{\mathrm{ML}} = u_{\mathrm{EL}} f_{\Lambda} + u_{\mathrm{I}} \left(1 - f_{\Lambda}\right) \tag{32}$$

$$f_{\Lambda} = 1.21\Lambda^{0.64} \Big/ \left(1 + 0.37\Lambda^{1.26}\right) \tag{33}$$

$$\Lambda = h_{\min} / R_{\mathrm{a}} \tag{34}$$

where f_{Λ} is the percentage of point contact load distribution, and $h_{\min}$ is the minimum oil film thickness that can be calculated as follows:

$$h_{\min} = 2.69 R U^{0.67} G^{0.53} W^{-0.67} \tag{35}$$

$$U = \frac{\eta v_{\mathrm{e}}}{ER} \tag{36}$$

$$G = \xi E \tag{37}$$

$$W = \frac{F_{\mathrm{n}}}{ER^2} \tag{38}$$

In the above equations, ξ is the viscous compression coefficient, E is the equivalent elastic modulus, F_{n} is the normal load of the tooth surface based on the dynamic meshing force, and η is the dynamic viscosity of lubricating oil.

Mixed lubrication occurs in the impact stage within the line of action, that is, in the process from the end of the impact outside the line to the reduction of the impact. In this stage, the lubrication state recovers from the initial impact friction state to the elastic lubrication state, and the time period is t_{I} to t_{s}.

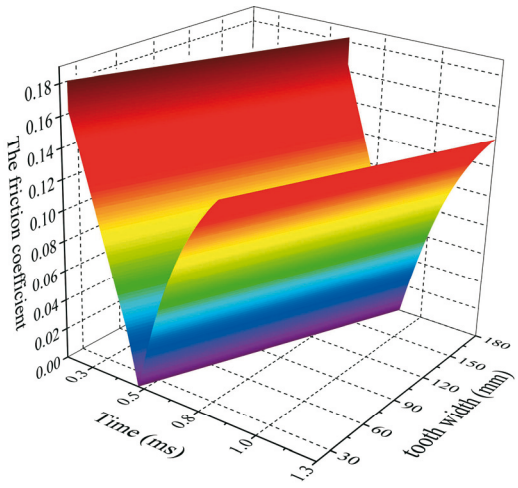

Fig. 9 The time-varying sliding friction coefficient of helical gear

The sliding friction coefficients of the three states are characterised to obtain the time-varying sliding friction coefficient of the helical gear, as shown in Fig. 9. Thus, the sliding friction force can be expressed as

$$F_{\mathrm{f}}(t) = \sum \mu_m(t) \frac{F_{\mathrm{n}}}{L_z(t)} \frac{\Delta x}{\cos\beta} \operatorname{sgn}\left(SR_m(t)\right) \tag{39}$$

$$\operatorname{sgn}\left(SR_m(t)\right) = \begin{cases} 1 & SR_m(t) > 0 \\ 0 & SR_m(t) = 0 \\ -1 & SR_m(t) < 0 \end{cases}, \tag{40}$$

where Δx represents the slice thickness, F_{n} is the normal force, and $L_z(t)$ is the time-varying contact line length.

The sliding friction force of the helical gear pair is calculated considering the gear impact. Figure 10(a) shows the sliding friction force of a single tooth pair. The maximum friction force without gear impact taken into consideration is 1563.5 N, and the maximum friction force with gear impact taken into consideration is 1778.4 N, which is an increase of 214.9 N. When the gear enters the meshing stage, the sliding friction coefficient of the gear increases due to the gear impact, which causes the sliding friction force of the helical gear to increase in the meshing stage.

Figure 10(b) shows the sliding friction force of the helical gear pair. The change laws of the friction excitation with and without gear impact taken into consideration are very similar. However, the sliding friction force of the gear increases because of the gear impact. When there is no gear impact on the gear pair, the friction force on one side of the pitch line is slightly greater than that on the other side. The friction forces on both sides of the pitch line can well offset each other. When the gear impact on the gear pair occurs, the friction forces on both sides of the pitch line are unbalanced because of it, and the sliding friction force of the helical gear increases, which, in turn, affects the stability of the gear transmission.

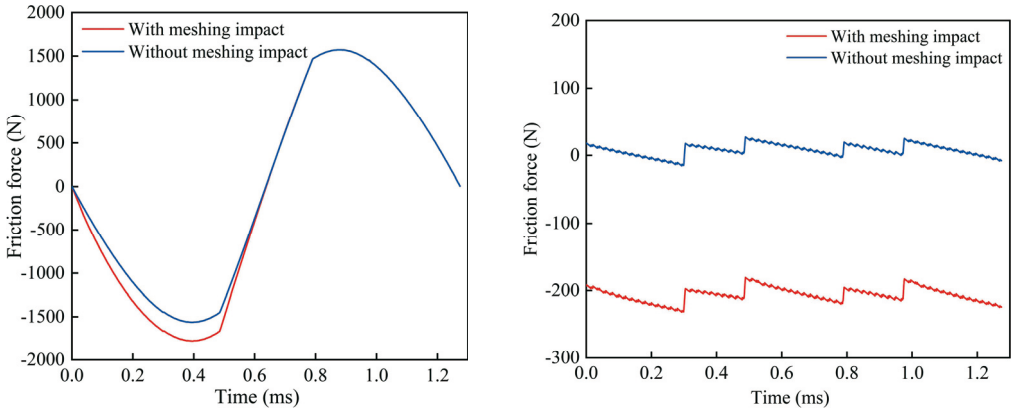

(a) A single tooth pair (b) A helical gear pair

Fig. 10 The sliding friction force

4.2 Calculation method of tooth surface load considering gear impact

Figure 11 shows a dynamic model of the helical gear transmission system considering gear impact. Gear 1 is the input end and T_1 is the input torque. Gear 2 is the output end, and T_2 is the output torque; k_m and c_m are the meshing stiffness and the meshing damping of the helical gear, respectively.

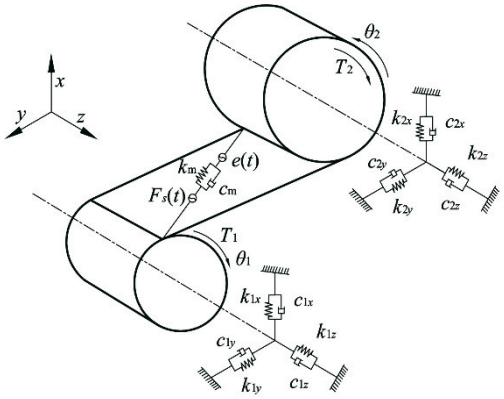

Fig. 11 Dynamic model of the helical gear transmission system

The stiffness calculation here uses the slice method. The stiffness of each piece of spur gear is calculated based on the potential energy method, using equations (41)-(46):

$$k_{\mathrm{m}i}=\frac{1}{\sum_{i=1}^{2}\left(\frac{1}{k_{\mathrm{b}i}}+\frac{1}{k_{\mathrm{s}i}}+\frac{1}{k_{\mathrm{a}i}}+\frac{1}{k_{\mathrm{f}i}}\right)+\frac{1}{k_{\mathrm{h}}}} \tag{41}$$

$$k_{\mathrm{b}}=\frac{1}{\int_{x_M}^{x(\alpha_z)}\frac{3\cos^2\beta[\cos\alpha_z(x(\alpha_z)-x)-\sin\alpha_z y(\alpha_z)]^2}{2Ey^3B/N}\mathrm{d}x} \tag{42}$$

$$k_{\mathrm{s}}=\frac{1}{\int_{x_M}^{x(\alpha_z)}\frac{0.6\cos^2\beta\cos^2\alpha_z}{GyB/N}\mathrm{d}x} \tag{43}$$

$$k_{\mathrm{a}}=\frac{1}{\int_{x_M}^{x(\alpha_z)}\frac{\cos^2\beta\sin^2\alpha_z}{2EyB/N}\mathrm{d}x} \tag{44}$$

$$k_{\mathrm{tf}}=\frac{B}{\frac{N\cos^2\beta\cos^2\alpha_z}{E}\left\{L^*\left(\frac{u_{\mathrm{f}}}{S_{\mathrm{f}}}\right)^2+M^*\left(\frac{u_{\mathrm{f}}}{S_{\mathrm{f}}}+P^*(1+Q^*\tan^2\alpha_z)\right)\right\}} \tag{45}$$

$$k_{\mathrm{h}}=\frac{\pi EB}{4N(1-\mu^2)}, \tag{46}$$

where α_z represents the pressure angle of the contact point; E, G, and μ are Young's modulus, the shear modulus, and Poisson's ratio, respectively; $x(\alpha_z)$ and $y(\alpha_z)$ are the coordinates of the contact point; B is the tooth width; L^*, M^*, P^*, and Q^* are listed in Ref [27].

The meshing damping of tooth pairs, c_{m}, is calculated by the following formula:

$$c_{\mathrm{m}}=2\xi\sqrt{\frac{k_{\mathrm{m}}r_{\mathrm{b1}}^2r_{\mathrm{b2}}^2J_1J_2}{r_{\mathrm{b1}}^2J_1+r_{\mathrm{b2}}^2J_2}}, \tag{47}$$

where J_1 and J_2 are the moment of inertia of the driving gear and the driven gear, respectively, k_{m} is the meshing stiffness, and ξ is the damping ratio with a value range of 0.03-0.17.

In the 8-DOF concentrated mass dynamics model of the high-speed and heavy-duty helical gear pair transmission system, x_i, y_i, and z_i represent the translational degrees of freedom of the gear, and θ_i represents the rotational freedom of the gear (i=1, 2); then, the generalised displacement array of the system is as follows:

$$\left\{x_1\ \ y_1\ \ z_1\ \ \theta_1\ \ \ x_2\ \ y_2\ z_2\ \ \theta_2\right\}^{\mathrm{T}}. \tag{48}$$

In the meshing process, the helical gear pair produces relative displacement in the normal direction of the meshing point, δ, which is expressed as

$$\begin{aligned}\delta=&-(x_1-x_2)\sin\alpha_{\mathrm{n}}+(y_1-y_2+r_1\theta_1-r_2\theta_2)\cos\alpha_{\mathrm{n}}\cos\beta\\&+\left(z_1-z_2\right)\cos\alpha_{\mathrm{n}}\sin\beta-e\left(t\right)\end{aligned}. \tag{49}$$

The dynamic meshing force, F_{n},, and the component force along each coordinate of the helical gear are:

$$\begin{cases} F_{\mathrm{n}} = k_{\mathrm{m}}\delta + c_{\mathrm{m}}\dot{\delta} \\ F_x = F_{\mathrm{n}} \sin\alpha_{\mathrm{n}} \\ F_y = F_{\mathrm{n}} \cos\alpha_{\mathrm{n}} \cos\beta \\ F_z = F_{\mathrm{n}} \cos\alpha_{\mathrm{n}} \sin\beta \end{cases} \tag{50}$$

Therefore, the vibration differential equation of the helical gear transmission gear system can be expressed as

$$\begin{cases} m_1\ddot{x}_1 + c_{1x}\dot{x}_1 + k_{1x}x_1 = F_{x1} \\ m_1\ddot{y}_1 + c_{1y}\dot{y}_1 + k_{1y}y_1 = F_{y1} \\ m_1\ddot{z}_1 + c_{1z}\dot{z}_1 + k_{1z}z_1 = F_{z1} \\ I_1\ddot{\theta}_1 = T_1 - F_{y1}r_{\mathrm{b1}} - F_{\mathrm{s}}r_{\mathrm{b1}} \\ m_2\ddot{x}_2 + c_{2x}\dot{x}_2 + k_{2x}x_2 = -F_{x2} \\ m_2\ddot{y}_2 + c_{2y}\dot{y}_2 + k_{2y}y_2 = -F_{y2} \\ m_2\ddot{z}_2 + c_{2z}\dot{z}_2 + k_{2z}z_2 = -F_{z2} \\ I_2\ddot{\theta}_2 = -T_2 + F_{y2}r_{\mathrm{b2}} + F_{\mathrm{s}}r_{\mathrm{b2}} \end{cases}, \tag{51}$$

where m_1 and m_2 are the masses of the driving and driven wheels, F_{s} is the meshing impact of the gear pair, k_{1i} and k_{2i} are the support stiffness of the driving and driven wheels, and c_{1i} and c_{2i} are the main and the driven wheel support damping, and i=x, y, z.

The equation set (51) is solved by varying the step four order Runge-Kutta method. The relative displacement of the helical gear pair in the normal direction at the meshing point δ is obtained. The tooth surface contact force with the gear impact considered is calculated by formula (52) given below, as shown in Fig 12(a). The spectrum of tooth surface contact force with the gear impact considered is obtained by the Fourier transform, as shown in Fig 12(b).

$$F = k_{\mathrm{m}}(t)\delta + c_{\mathrm{m}}\dot{\delta} + F_s \tag{52}$$

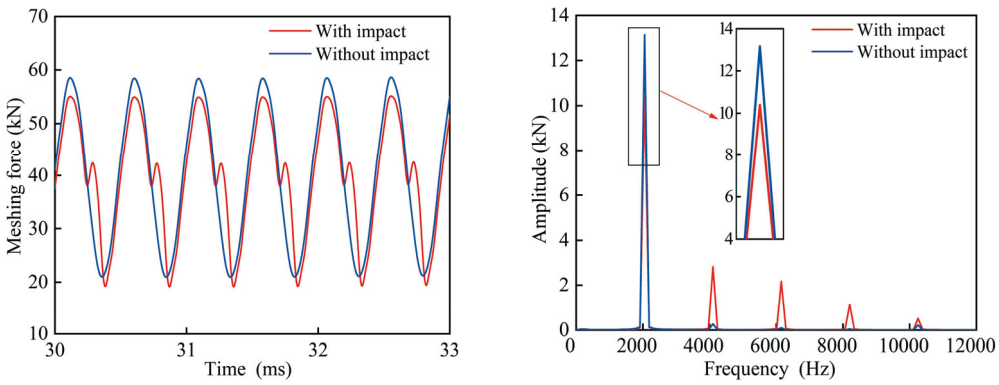

(a) Time history (b) FFT spectrum

Fig. 12 Contact force of the helical gear pair

As shown in Fig.12(a), the gear impact increases the average value of the tooth surface contact force by 0.26% and reduces the amplitude of the tooth surface contact force by 3.47%. Therefore, the gear impact has little effect on the gear bearing capacity. Since the phase of the gear impact force is the same at the second, the third, and the fourth frequency of the meshing frequency (Fig. 12(b)), the gear impact increases the corresponding amplitude of the contact force. At the meshing frequency, the phase of the contact force is opposite to the impact phase of the gear, so the amplitude of the contact force decreases.

5. Conclusions

Since the multi-tooth impact and the temperature effect are not considered in the analytical model of the impact force of a high-speed helical gear pair, an analytical calculation method for the high-speed helical gear multi-tooth impact excitation under the temperature effect is proposed here, based on the principle of conservation of energy. In addition, the influence of gear impact on the sliding friction force and the tooth surface contact force is studied [28]. The conclusions are as follows:

(1) The analytical formula for the meshing impact of a helical gear pair considering the temperature effect is derived. From the comparison of the calculation results, one can see that the tooth surface temperature increases the impact excitation of the helical gear pair, and the temperature has a great influence on the meshing impact of the helical gear pair and has a weak influence on tooth pair II and tooth pair III.

(2) Based on the principle of energy conservation, the calculation method of multi-tooth impact excitation of a helical gear pair is obtained. The influence of different gear parameters on the multi-tooth impact force of the involute helical gear pair is studied. With the increase in the speed and torque, the impact force of different tooth pairs increases. With the increase of the gear module, the impact force of the first tooth increases, and the impact forces of the second and third teeth decrease. The influence of the three variables on the first tooth is greater than that on the other two teeth.

(3) The influence of gear impact excitation on the sliding friction force and the tooth surface contact force is studied. The gear impact increases the sliding friction force of the gears in the meshing stage, resulting in the increase in the sliding friction force. The gear impact has little effect on the gear bearing capacity, but the amplitude of the contact force at the meshing frequency is reduced, and the amplitude of the contact force at the second, third, and fourth frequencies of the meshing frequency is increased. The multi-tooth impact decreases the amplitude of the first mesh harmonic and increases the amplitude of the second, third, and fourth mesh harmonics.

REFERENCES

[1] R. Yang, B. Han and J. Xiang, "Nonlinear dynamic analysis of a trochoid cam gear with the tooth profile modification," Int. J. Precis. Eng. Manuf., vol. 21, no. 12, pp. 2299-2321, Oct. 2020. https://doi.org/10.1007/s12541-020-00417-6

[2] Z. Chen, J. Ning, K. Wang and W. Zhai, "An improved dynamic model of spur gear transmission considering coupling effect between gear neighboring teeth," Nonlinear Dyn, vol. 106, no. 1, pp. 339-357, Sep. 2021. https://doi.org/10.1007/s11071-021-06852-y

[3] M. Aleksandar and M. Banić. "Thermal analysis of a crossed helical gearbox using FEM," Transactions of FAMENA. vol. 44, no. 1, pp.67-78, May. 2020. https://doi.org/10.21278/TOF.44106

[4] G. Ignacio and F. Alfonso, "Implementation of a finite element model for stress analysis of gear drives based on multi-point constraints," Mech. Mach. Theory, vol. 117, pp. 35-47, Nov. 2017. https://doi.org/10.1016/j.mechmachtheory.2017.07.005

[5] M. Bryant, H. Evans and R. Snidle, "Plastic deformation in rough surface line contacts-a finite element study," Tribology International, vol. 46, no. 1, pp. 269-278, Feb. 2012. https://doi.org/10.1016/j.triboint.2011.06.024

[6] Z. Zhang, Z. Fong, Y. Li and H. Fang, "A study of the contact stress analysis of cylindrical gears using the hybrid finite element method," Proc. Inst. Mech. Eng. C: J. Mech. Eng. Sci, vol. 227, pp. 3-18, Apr. 2012. https://doi.org/10.1177/0954406212444383

[7] T. Lin and Z. He, "Analytical method for coupled transmission error of helical gear system with machining error," assembly errors and tooth modifications, Mech. Syst. Signal Process, vol. 91, pp. 167-182, Jul. 2017. https://doi.org/10.1016/j.ymssp.2017.01.005

[8] W. Cheng, "Study on 3-D modification for reducing vibration of helical gear based on TCA technology, LTCA technology and system dynamics," Mech. Syst. Signal Process, vol. 146, pp. 106991, Jan. 2021. https://doi.org/10.1016/j.ymssp.2020.106991

[9] B. Marco, Z. Antonio and P. Francesco, "Adaptive grid-size finite element modeling of helical gear pairs," Mech. Mach. Theory, vol. 82, pp. 17-32, Dec. 2014. https://doi.org/10.1016/j.mechmachtheory.2014.07.009

[10] P. Ziegler and P. Eberhard, "Simulative and experimental investigation of impacts on gear wheels," Comput. Methods Appl. Mech. Engrg, vol. 197, pp. 4653-4662, Oct. 2008. https://doi.org/10.1016/j.cma.2008.06.007

[11] J. Tang, W. Zhou and S. Chen, "Contact-impact analysis of gear transmission system," Chin. J. Mech. Eng, vol. 47, no. 7, pp. 22-30, Jan. 2011. https://doi.org/10.3901/JME.2011.07.022

[12] D. Ma, Y. Liu, Z. Ye and Y. Wei, "Meshing contact impact properties of circular arc tooth trace cylindrical gear based on rotating knife dish milling process," Mathematical Problems in Engineering, pp. 8819818, Jan. 2021. https://doi.org/10.1155/2021/8819818

[13] R. Imin and M. Geni, "Stress analysis of gear meshing impact based on SPH method," Mathematical Problems in Engineering, vol. 4, pp. 1-7, Apr. 2014. https://doi.org/10.1155/2014/328216

[14] F. Guo and Z. Fang, "A new algorithm to solve meshing-in impact considering the measured pitch error and to investigate its influence on the dynamic characteristics of a gear system," Int. J. Precis. Eng. Manuf, vol. 20, no. 3, pp. 395-406, Feb. 2019. https://doi.org/10.1007/s12541-019-00047-7

[15] S. Hu, Z. Fang, C. Liu and L. Xiang, "Measurements and theoretical analysis of a helical gear meshing impact signal," Proc. IME K J. Multi-body Dyn, vol. 233, no. 4, pp. 827-839, Jun. 2019. https://doi.org/10.1177/1464419319853435

[16] Y. Mu, Z. Fang and W. Li, "Impact analysis and vibration reduction design of spiral bevel gears," Proc. IME K J. Multi-body Dyn, vol. 233, no. 3, pp. 668-676, Mar. 2019. https://doi.org/10.1177/1464419319827398

[17] C. Zhou and S. Chen, "Modeling and calculation of impact friction caused by corner contact in gear transmission," Chin. J. Mech. Eng, vol. 27, no. 5, pp. 958-964, Aug. 2014. https://doi.org/10.3901/CJME.2014.0616.110

[18] I. D. Atanasovska and K. R. Hedrih. "A new collision model for analysing the vibro-impact of spur gears," Transactions of FAMENA. vol. 42, no. 2, pp.1-13, Jul. 2018. https://doi.org/10.21278/TOF.42201

[19] Y. Li, B. Wu and L. Zhu, "Analysis and calculation of double circular arc gear meshing impact model," Open Mech. Eng. J, vol. 9, no. 1, pp. 160-167, 2015. https://doi.org/10.2174/1874155X01509010160

[20] Z. HE, T. Zhang and T. Lin, "Novel mathematical modelling method for meshing impact of helical gear," Mech. Mach. Theory, vol. 152, pp. 103949, Oct. 2020. https://doi.org/10.1016/j.mechmachtheory.2020.103949

[21] J. Yang, T. Lin, Z. He and M. Chen, "Novel calculation method for dynamic excitation of modified double-helical gear transmission," Mech. Mach. Theory, vol. 167, pp. 104467, Jan. 2022. https://doi.org/10.1016/j.mechmachtheory.2021.104467

[22] A. Miltenovic, M. Banic, J. Tanaskovic, et al. "Wear load capacity of crossed helical gears." Facta Universitatis, Series: Mechanical Engineering, vol. 22, no. 1, pp.125-138, Apr. 2024. https://doi.org/10.22190/FUME220114015M

[23] X. Gou, L. Zhu and C. Qi, "Nonlinear dynamic model of a gear-rotor-bearing system considering the flash temperature," J. Sound Vib, vol. 410, no. 1, pp. 187-208, Dec. 2017. https://doi.org/10.1016/j.jsv.2017.08.014

[24] H. Xu, A. Kahraman and N. Anderson, "Prediction of mechanical efficiency of parallel-axis gear pairs," J. Mech. Design, vol. 129, no. 1, pp. 58-68, Jun. 2006. https://doi.org/10.1115/1.2359478

[25] P. Anuradha and P. Kumar, "Effect of lubricant selection on EHL performance of involute spur gears," J. Tribol. Int, vol. 50, no. 4, pp. 82-90, Jun. 2012. https://doi.org/10.1016/j.triboint.2012.02.006

[26] V. Simon, "Multi-objective optimization of hypoid gears to improve operating characteristics," Mech. Mach. Theory, pp.103727, 2020. https://doi.org/10.1016/j.mechmachtheory.2019.103727

[27] P. Sainsot, P. Velex, O. Duverger, "Contribution of gear body to tooth deflections-a new bidimensional analytical formula," J. Mech. Design, vol.126, pp.748-752, 2004. https://doi.org/10.1115/1.1758252

[28] Z. Vrcan, S. Troha, K. Marković, et al. "Analysis of complex planetary gearboxes." Spectrum of Mechanical Engineering and Operational Research, vol. 1, no. 1, pp.227-49. Sep. 2024. https://doi.org/10.31181/smeor11202420

Submitted: 31.8.2024

Accepted: 05.5.2025

Zhen Yang*
State key Laboratory of Mechanical transmission, Chongqing University, No.174 Sha Jie, ShaPingBaQu District, Chongqing 400044, China and Chongqing Gearbox Co., Ltd., Jiangjin District Chongqing 402263, China

Qian Tang
State key Laboratory of Mechanical transmission, Chongqing University, No.174 Sha Jie, ShaPingBaQu District, Chongqing 400044, China

Dong Peng
School of Mechatronics & Vehicle Engineering, Chongqing Jiaotong University, No.66 Xuefu Road, Nan'an District, Chongqing 400074, China

Zeyin He
School of Mechatronics & Vehicle Engineering, Chongqing Jiaotong University, No.66 Xuefu Road, Nan'an District, Chongqing 400074, China and State key Laboratory of Mechanical transmission, Chongqing University, No.174 Sha Jie, ShaPingBaQu District, Chongqing 400044, China

Chun Gan
School of Mechatronics & Vehicle Engineering, Chongqing Jiaotong University, No.66 Xuefu Road, Nan'an District, Chongqing 400074, China

*Corresponding author:
760698776@qq.com